Liquid Crystals
Publication details, including instructions for authors and subscription information:
http://www.informaworld.com/smpp/title~content=t713926090

Phase diagram and electro-optical Kerr effect of nematic mixtures containingtolane and biphenyl cores

A. Ghanadzadeh Gilani[ab]; H. Tajalli[a]; A. Vahedi[a]
[a] Center of Applied Physics and Astronomy, Tabriz University, Tabriz, Iran [b] Department of Chemistry, Faculty of Science, University of Guilan, Rasht, Iran

To cite this Article Ghanadzadeh Gilani, A. , Tajalli, H. and Vahedi, A.(2009) 'Phase diagram and electro-optical Kerr effect of nematic mixtures containingtolane and biphenyl cores', Liquid Crystals, 36: 4, 347 — 352
To link to this Article: DOI: 10.1080/02678290902893761
URL: http://dx.doi.org/10.1080/02678290902893761

Liquid Crystals,
Vol. 36, No. 4, April 2009, 347–352

Taylor & Francis
Taylor & Francis Group

Phase diagram and electro-optical Kerr effect of nematic mixtures containing tolane and biphenyl cores

A. Ghanadzadeh Gilani[a,b]*, H. Tajalli and A. Vahedi[a]

[a]*Center of Applied Physics and Astronomy, Tabriz University, Tabriz, Iran;* [b]*Department of Chemistry, Faculty of Science, University of Guilan, Rasht, Iran*

(Received 15 February 2009; final form 13 March 2009)

An experimental phase diagram for two types of nematic liquid crystals and their binary mixtures was established by polarised optical microscopy and differential scanning calorimetry methods. The mixtures comprised a tolane-base liquid crystal, 4-heptyl-3-fluoro-4-isothiocyanatotolane (7TOLF), and a biphenyl-base nematogen, 4-heptyl-3-fluoro-4-isothiocyanatobiphenyl (7BF). The static Kerr effect and third-order non-linearity were investigated for 7TOLF and 7BF and their nematic mixtures within the isotropic phase. Both the compounds have a positive and large Kerr constant. The second-order phase-transition temperatures, T^*, were determined for these mixtures. The linear dependence of $(T - T^*)^{-1}$ on the Kerr constant is found to be in good agreement with the predications of the Landau–de Gennes model. The third-order non-linear susceptibility, $\chi^{(3)}$, values were determined for these mixtures.

Keywords: liquid crystals; nematic mixture; electro-optic Kerr effect; pre-transition behaviour

1. Introduction

Nematic liquid crystals (LCs) are unique in their properties and uses. Materials with nematic liquid crystalline properties possess large optical anisotropy owing to their large molecular anisotropy and intermolecular ordering (*1*). These materials are applied in many technical applications such as electro-optical displays, optical storage devices and non-linear optics. Therefore, the design of stable LC materials having high birefringence and low viscosity is always needed in the wide range of electro-optic applications. To achieve high optical anisotropy, highly conjugated LC compounds are usually desirable candidates (*2–4*). Unfortunately, increasing birefringence is associated with a high melting temperature and an increased viscosity. However, these problems can be overcome through the use of eutectic mixtures (*5*).

In recent years, the physical properties of nematic mixtures have received much attention. This interest is due to their desirable liquid crystalline range, optical and electro-optical properties. The physical properties of a nematic mixture depend on those of the components used and their relative concentrations. It is highly desirable to formulate a nematic mixture with high birefringence, low clearing temperature and low viscosity, which are the most critical parameters. The electro-optical behaviour of a number of nematic mixtures in the isotropic phase has been studied by many researchers (*6–10*).

In this investigation we are concerned with mixtures of two LCs of the high birefringence nematic type with positive dielectric anisotropy. They are 4-heptyl-3-fluoro-4-isothiocyanatobiphenyl (7BF) and 4-heptyl-3-fluoro-4-isothiocyanatotolane (7TOLF). The mixtures are characterised by components having a polar isothiocyanate terminal group at one side and the alkyl group at the other side. Both the compounds have a fluorine atom attached to the phenyl ring and exhibit only the nematic phase (Figure 1). The investigation reported here is concerned with the determination of the Kerr constant and the third-order non-linearity of mixtures of 7BF and 7TOLF in the isotropic state. The temperature dependencies of the Kerr effect data of the pure compounds 7BF and 7TOLF have been reported in one of our earlier publications (*11*).

Optical anisotropy (birefringence) is one of the most convenient and sensitive parameters for investigating and characterising the molecular anisotropy and intermolecular ordering in liquid crystals (*12–15*). The birefringence, Δn, of a medium is defined as the difference between the refractive indices for light polarised parallel ($n_{||}$) and perpendicular ($n_{\perp}$) to the orienting field direction, i.e. $\Delta n = n_{ll} - n_{\perp}$. The induction of birefringence in a fluid by application of an external electric field is known as the electro-optical Kerr effect (*16*), which depends both on polarity and polarisability (optical and electrical) of the molecules. Measurements of the temperature dependence of the Kerr effect in the isotropic phase, and pre-transitional behaviour, related to order parameter fluctuations, of many nematic LCs, have been studied (*17–20*). In the majority of publications, a

---

*Corresponding author. Email: aggilani@guilan.ac.ir

ISSN 0267-8292 print/ISSN 1366-5855 online

DOI: 10.1080/02678290902893761
http://www.informaworld.com

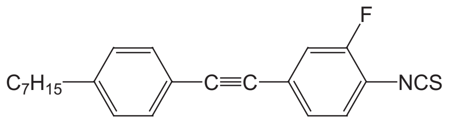

4`-heptyl-3-fluoro-4isothiocyanatotolane

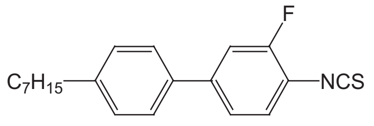

4`-hepty-3-fluoro-4isothiocyanatobiphenyl

Figure 1. Structures of the nematic compounds studied in this work.

good agreement between experimental and mean-field theory for nematic compounds was reported and discussed. Also, the third-order non-linear susceptibility, which is an important material parameter, can be obtained using Kerr effect measurements (*13*).

2. Experimental procedure

2.1 Materials

The pure nematic compounds 7BF and 7TOLF were synthesised at the Institute of Chemistry of the Military Technical Academy, Warsaw, Poland (*4*). The pure nematic compounds which were selected for the investigations are displayed in Figure 1. Several test nematic mixtures were prepared for this study. The clearing points or nematic-to-isotropic transition temperatures for these compounds were measured using differential scanning calorimetry (DSC) and polarising microscopy (POM) methods.

2.2 Kerr effect apparatus

A diagram of the experimental setup used to measure the electrically induced phase difference is illustrated in Figure 2. In this study, a He–Ne laser emitting at a wavelength of 632.8 nm with a power of 5 mW was used as a light source. The sample holder was a quartz spectrophotometer cell with a path length of 10 mm. The stainless steel electrodes were inserted into the Kerr cell, leaving an active column of liquid $2 \times 2 \times 10$ mm^3. A Teflon spacer was used to provide insulation between the electrodes and to maintain an electrode gap of 2 mm. The lower part of the Kerr cell was fitted into a thermostatted metal jacket, which was cut away to allow passage of the light beam. The temperatures were determined with a copper–constantan thermocouple.

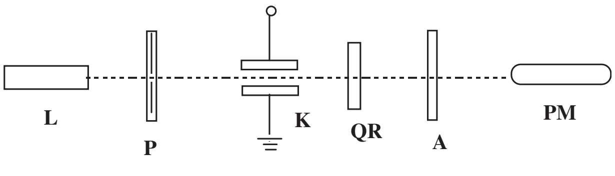

Figure 2. Diagram of apparatus used to measure the electro-optical Kerr effect. Principle components are: L, laser; P, Polariser; K, Kerr cell; QR, quarter-wave retarder; A, analyser; PM, photomultiplier.

Detection of the Kerr signal was achieved using a photomultiplier tube, type E.M.I. 9816B. The optical signal from the photomultiplier was displayed using a digital storage oscilloscope and a PC computer. The polariser and analyser were Glan–Thompson double refraction type prisms of commercial origin and adjusted such that they crossed each other, making an angle of 45° with respect to the applied AC field (1 kHz). The quarter wave plate used in these experiments was mica cut specifically for use at 632.8 nm and mounted between glass discs. The electric field is generated by means of a high-voltage power supply that was applied, as a short duration rectangular-shaped pulse from a pulse generator, to the electrodes of the Kerr cell.

All measurements of the Kerr constant were made using the nulled intensity method (*21*), which involves the nulling of an optical response resulting from the application of a short-duration rectangular-shaped electric field across the Kerr cell. In the absence of the applied electric field, the intensity of the light detected by the photomultiplier is given by

$$I = I_o \sin^2 \alpha \qquad (1)$$

where α is the rotation of the analyser with respect to the nulled condition and is the maximum intensity of the probe beam when the polariser and analyser are completely uncrossed. On application of an electric field, the intensity of the light falling on the photomultiplier when the medium becomes birefringent is given by

$$I = I_o \sin^2(\alpha + \delta/2) \qquad (2)$$

3. Results and discussion

3.1 Phase diagrams of the mixtures

In this investigation we are concerned with two types of nematic LCs containing tolane and biphenyl cores. Both the compounds have a fluorine atom attached to the phenyl ring and exhibit only the nematic phase. Owing to the lateral fluorine atom, these nematic LCs exhibit a relatively low clearing temperature. The compounds which were selected for this study are presented in Figure 1.

Table 1. The clearing temperature, T_C, and pre-transitional temperature, T^*, of the mixtures.

Compound	$T_C\,(^\circ C)$	$T_C^*(^\circ C)$
7TOLF (100%)	43.4	42.3
F1: 7BF/7TOLF (40/60)	38.4	37.6
F2: 7BF/7TOLF (50/50)	37.3	36.4
F3: 7BF/7TOLF (60/40)	36.2	35.0
F4: 7BF/7TOLF (70/30)	34.6	33.5
F5: 7BF/7TOLF (80/20)	33.1	32.0
7BF (100%)	30.4	29.2

By changing the ratio of the pure compounds, we prepared some test nematic mixtures. The phase transition temperatures for the pure compounds (7TOLF and 7BF) and their binary mixtures were measured using DSC and POM methods during the cooling runs. Their corresponding phase transition temperatures are listed in Table 1. Figure 3 demonstrates the experimental phase diagram of the 7BF/7TOLF system. As can be seen in Figure 3, the clearing temperatures of the binary mixtures vary linearly with composition and a eutectic behaviour is illustrated. The eutectic nematic mixture of F_1 (40% 7BF + 60% 7TOLF) shows a broad nematic range ($\Delta T = 64.2$K) in the cooling cycle.

3.2 *Kerr effect in mixtures of 7BF and 7TOLF*

The electric field induced birefringence, Δn, which increases proportionally to the square of the electric field **E**, may be defined by (Kerr law):

$$\Delta n = \lambda B E^2. \tag{3}$$

Where λ is the wavelength of the light, and B is the 'Kerr constant' of the substance, and is used to denote the magnitude of the Kerr effect. The induced birefringence may be measured by detecting the optical phase difference, δ, between waves of the two polarisations upon passage through a medium made birefringent by an electric field.

$$\delta = 2\pi l B E^2 = 2\pi l \Delta n / \lambda \tag{4}$$

where l is the optical path length of the Kerr cell. For the nulled intensity method of measuring the Kerr effect, which involves the nulling of an optical response resulting from the application of an external electric field across the Kerr cell, the rotation of the plane of polarisation, α, is related to the phase difference, δ, by $\alpha = \delta/4$. Eliminating δ from Equation (4) and rearranging gives $\alpha = \pi L B E^2/2$. If the Kerr law is observed, a plot of α versus the square of applied electric field also should give a straight-line graph passing through the origin with a gradient of $(\pi L B/2)$, from which the Kerr constant B may be determined.

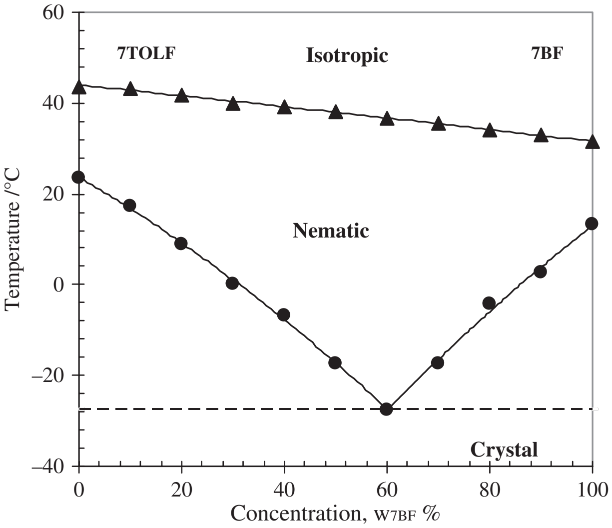

Figure 3. Phase diagram of the mixture 7BF/7TOLF.

In this work, we prepared five high birefringence and low clearing temperature LC nematic mixtures for the electro-optical investigation in the isotropic phase. These mixtures were designated as F_1, F_2, F_3, F_4 and F_5. The Kerr constant, B, of a material at a given temperature may be obtained from the gradient of a graph of induced birefringence, Δn, plotted against the square of applied electric field (i.e. $\Delta n = \lambda B E^2$). For each of the materials, the electrically induced birefringence was found to be a linear function of the square of the applied electric field and is positive in all cases ($\Delta n > 0$). For a comparison, the Kerr constants of the mixtures measured at different temperatures in the isotropic phase are summarised in Table 2. The dependences of the Kerr constant, B, on temperature for the pure compounds and for the nematic mixtures are shown in Figure 4. These data show that the values of B depend strongly on temperature and those of the components used and their relative concentrations. The Kerr constants of these liquid crystalline mixtures are found to be very high in the isotropic phase. This may be due to presence of high polarisable tolane and biphenyl cores and polar–NSC group, which are conductive to high optical anisotropy.

The theory of Landau–de Gennes (*22*) has been used to describe the pre-transitional behaviour in the isotropic phase of LCs. This theory is essentially based on the assumption that short-range forces predominate in the region of the nematic–isotropic transition. According to this model the Kerr constant in the isotropic phase is given by

$$B = \frac{\varepsilon_o \Delta n_o \Delta \varepsilon_o}{4a\lambda\sqrt{\varepsilon}(T - T^*)}. \tag{5}$$

Table 2. Kerr constants, *B*, and susceptibility, $\chi^{(3)}$, of the mixtures, for $\lambda = 632.8$ nm.

Temp. (°C)	10^{11} B/mV^{-2}	B^{-1}/10^{11}m^{-1}V^{2}	$10^{18}\chi^{(3)}$/m^{2}V^{-2}
F_1: 7BF/7TOLF (40/60)			
39.00	18.91	0.05	2.57
39.20	17.14	0.06	2.34
39.40	15.68	0.06	2.14
39.60	13.44	0.07	1.84
39.80	12.26	0.08	1.67
40.00	11.96	0.08	1.63
41.49	7.24	0.14	0.99
42.57	5.65	0.18	0.77
44.73	3.90	0.26	0.53
49.00	2.48	0.40	0.34
F_2: 7BF/7TOLF (50/50)			
37.90	17.12	0.06	2.33
38.20	14.47	0.07	1.97
38.40	12.96	0.08	1.77
38.80	11.40	0.09	1.55
39.40	8.82	0.11	1.20
40.90	5.59	0.18	0.76
41.90	4.71	0.21	0.64
43.90	3.40	0.29	0.46
48.90	2.08	0.48	0.28
F_3: 7BF/7TOLF (60/40)			
36.70	14.11	0.07	1.92
36.80	12.31	0.08	1.68
37.00	11.30	0.09	1.54
37.40	10.55	0.09	1.44
38.90	5.74	0.17	0.78
40.20	4.29	0.23	0.58
42.00	3.36	0.30	0.46
44.20	2.46	0.41	0.33
46.40	2.05	0.49	0.28
F_4: 7BF/7TOLF (70/30)			
35.10	13.75	0.07	1.83
35.20	12.76	0.08	1.75
35.30	12.00	0.08	1.63
35.50	10.86	0.09	1.48
36.10	8.33	0.12	1.13
37.00	6.09	0.16	0.83
38.10	4.67	0.21	0.63
39.00	3.90	0.26	0.53
41.00	2.86	0.35	0.39
44.50	1.99	0.50	0.27
F_5: 7BF/7TOLF (80/20)			
33.60	13.30	0.08	1.78
33.70	12.45	0.08	1.70
33.80	12.00	0.08	1.63
34.00	10.44	0.10	1.42
34.60	7.94	0.13	1.08
36.15	5.00	0.20	0.68
37.10	4.06	0.25	0.55
39.30	2.78	0.36	0.38
41.90	2.11	0.47	0.29
33.60	13.30	0.08	1.78

Where a is the temperature independent coefficient, T^* is the second-order pre-transitional temperature, which is an extrapolated temperature just below the isotropic–nematic phase transition, and $\Delta\varepsilon_o$ is the low-frequency dielectric anisotropy in the completely ordered phase. From the above equation, there is a reciprocal relationship between the Kerr constant, *B*, and temperature as follows:

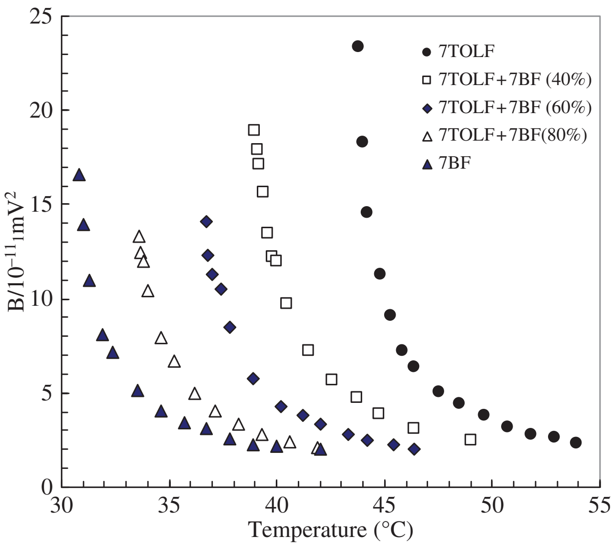

Figure 4. Temperature dependence of B for the nematic mixtures obtained using the pulsed AC field method (f = 1 kHz).

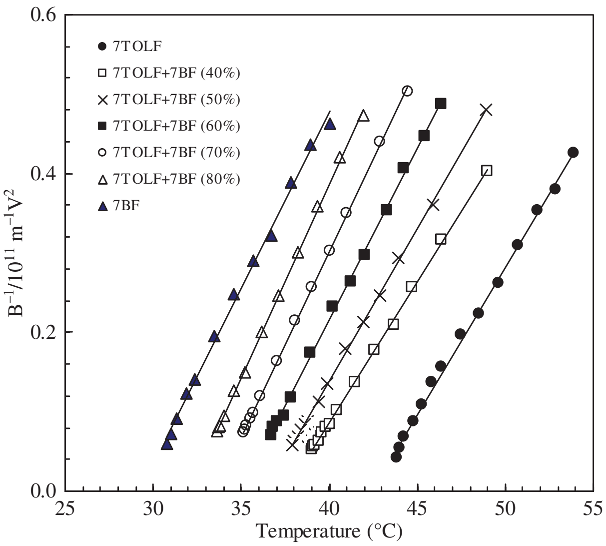

Figure 5. Temperature dependence of B^{-1} for the nematic mixtures obtained using the pulsed AC field method.

$$B \propto (T - T^{*})^{-\gamma} \tag{6}$$

where T^* is the second-order pre-transitional temperature. T^* can be obtained by a linear extrapolation of the Kerr constant (B^{-1}) versus temperature. γ is a numerical factor that equals unity in the Maier–Saupe theory.

In Figure 5, the inverse of the Kerr constant, B^{-1}, for the compounds is shown and compared as a function of temperature. For the samples studied the inverse of the Kerr constant varies linearity with temperature, i.e. $\gamma \cong 1$, as predicted by the Maier–Saupe mean-field theory for LCs (*23*). The samples display a Kerr response which obeys the Landau–de Gennes model in an ideal way. The extrapolated temperature T^* is found in all cases to be located approximately 1°C below the clearing temperatures of the mixtures. The pre-transitional temperature, T^*, and the clearing temperatures observed for the mixtures of different weight fractions are shown in Figure 6.

The electro-optical Kerr effect is used to determine the third-order non-linear susceptibility tensor $\chi^{(3)}$. The Kerr constant can be related to the susceptibility tensor in an isotropic media using the following formula (*24*):

$$B = \frac{24\pi}{n\lambda}\chi^{(3)} \tag{7}$$

where n is the refractive index of the nematic compound at a given temperature and λ is wavelength of the light. The susceptibility data of the mixtures measured at different temperatures in the isotropic phase are also summarised in Table 2. In general, the mixtures exhibit similar non-linearity behaviour. Figure 7 shows the variation of the susceptibility with temperature for the nematic mixtures in the isotropic phase.

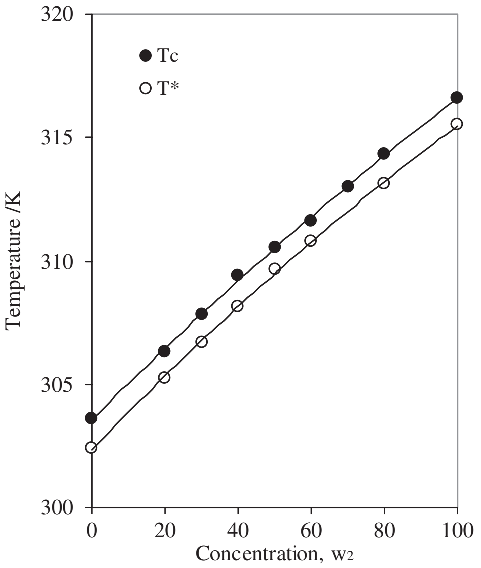

Figure 6. Change in nematic-isotropic transition temperature and second order pre-transitional temperature with weight fraction of 7BF in 7TOLF.

4. Conclusions

The values of the Kerr constants and susceptibilities were obtained for 7BF, 7TOLF and their nematic mixtures in the isotropic phase. These mixtures exhibit high birefringence and large non-linear

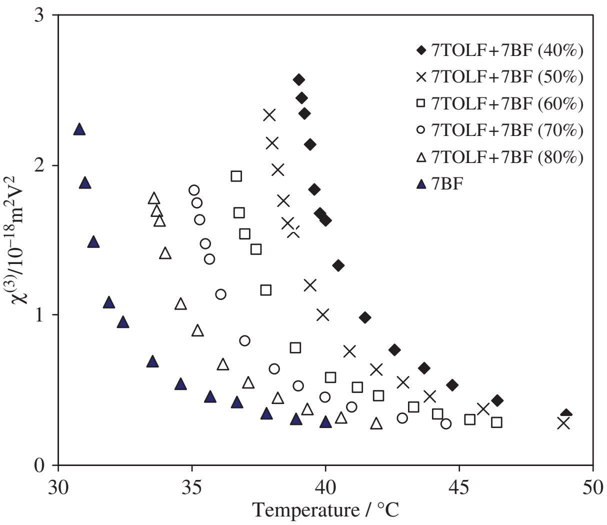

Figure 7. Variation of susceptibility for the nematic mixtures.

susceptibility. This is a consequence of the presence of highly polarisable tolane and biphenyl cores and polar NSC group, which are conductive to high optical anisotropy. The second-order phase-transition temperatures, *T**, were also determined for these compounds. In the pre-transition region the short-range order leads to pseudo-nematic domains of highly correlated molecules in the isotropic phase. The studied mixtures display pre-transitional effects within the isotropic phase close to the nematic phase which can be accounted for on the basis of the Landau–de Gennes model.

References

(1) Khoo, I.C.; Wu, S.T. *Optics and Nonlinear Optics of Liquid Crystals*; World Scientific: Singapore, 1993.
(2) Wu, S.T.; Efron, U.; Hess, L.D. *Appl. Opt.* **1984**, *23*, 3911–3915.
(3) Gauza, S.; Wen, C.H.; Wu, S.T.; Janarthanan, N.; Hsu, C.S. *Jpn. J. Appl. Phys.* **2004**, *43*, 7634–7638.
(4) Spadlo, A.; Dabrowski, R.; Filipowicz, M.; Stolarz, Z.; Przedmojski, J.; Gauza, S.; Fan, Y.H.; Wu, S.T. *Liq. Cryst.* **2003**, *30*, 191–198.
(5) Goto, Y.; Ogawa, T.; Sawada, S.; Sugimori, S. *Mol. Cryst. Liq. Cryst*. **1991**, *209*, 1–7.
(6) Ghanadzadeh, A.; Beevers, M.S. *J. Mol. Liq.* **2004**, *112*, 141–145.
(7) Philip, J.; Prasada Rao, T.A. *J. Mol. Liq.* **1991**, *50*, 215–223.
(8) Philip, J.; Prasada Rao, T.A. *J. Phys. D: Appl. Phys.* **1992**, *25*, 1231–1234.
(9) Schneider, L.; Wendorff, J.H. *Liq. Cryst*. **1997**, *22*, 29–35.
(10) Tajalli, H.; Ghanadzadeh, A.; Khoshsima, H.; Zhalefar, P. *Opto-Electron. Rev.* **2008**, *16*, 386–389.
(11) Khoshsima, H.; Tajalli, H.; Ghanadzadeh Gilani, A.; Dabrowski, R. *J. Phys. D: Appl. Phys*. **2006**, *39*, 1495–1499.
(12) Coles, H.J. *Mol. Cryst. Liq. Cryst*. **1978**, *49*, 67–74.
(13) Sinha, A.; Prasada Rao, T.A. *Liq. Cryst*. **2000**, *27*, 191–194.
(14) Khoshsima, H.; Tajalli, H.; Ghanadzadeh, A.; Dabrowski, R. *Mol. Cryst. Liq. Cryst.* **2006**, *46*, 93–106.
(15) Beevers, M.S. *Mol. Cryst. Liq. Cryst.* **1975**, *31*, 333–348.
(16) Kerr, J. *Phil. Mag*. **1875**, *50*, 337–348.
(17) Davies, M.; Moutran, R.; Price, A.H.; Beveers, M.S.; Williams, G. *J. Chem. Soc. Faraday Trans.* **1976**, *2*, 1447–1458.
(18) Philip, J.; Prasada Rao, T.A. *Phys. Rev. A* **1992**, *46*, 2163–2165.
(19) Coles, H.J.; Kershaw, S.V. *Mol. Cryst. Liq. Cryst. Lett*. **1985**, *2*, 29–35.
(20) Coles, H.J.; Kershaw, S.V. *J. Chem. Soc. Faraday Trans*. **1988**, *2*, 987–996.
(21) Beevers, M.S.; Khanarian, G. *Aus. J. Chem.* **1979**, *3*, 263–269.
(22) de Gennes, P.G. *Mol. Cryst. Liq. Cryst*. **1971**, *12*, 193–214.
(23) Maier, W.; Saupe, A. *Z. Naturforsch*. **1959**, *14a*, 882–900.
(24) Wang, C.C. *Phys. Rev*. **1966**, *152*, 149–156.